

Native extracellular matrix probes to target patient- and tissue- specific cell-microenvironment interactions by force spectroscopy

H. Holuigue¹, L. Nacci², P. Di Chiaro², M. Chighizola¹, I. Locatelli⁴, C. Schulte^{1,3,*}, M. Alfano^{4,*}, G.R. Diaferia^{2,*}, A. Podestà^{1,*}

¹ CIMAINA and Dipartimento di Fisica “Aldo Pontremoli”, Università degli Studi di Milano, , Milano, Italy.

² Department of Experimental Oncology, IEO, European Institute of Oncology IRCCS, Milano, Italy.

³ Department of Biomedical and Clinical Sciences "L. Sacco", Università degli Studi di Milano, Milano, Italy.

⁴ Division of Experimental Oncology/Unit of Urology, URI, IRCCS San Raffaele Hospital, Milan, Italy.

*Corresponding authors: carsten.schulte@unimi.it, alfano.massimo@hsr.it, giuseppe.diaferia@ieo.it, alessandro.podesta@mi.infn.it.

Supporting Information

Contents

Figure S1. Schematics of the conventional use of the LMD system.	2
Figure S2. Optical images of the ECM rat bladder.....	3
Figure S3. Stress tests on the ECM probes.	4
Figure S4. Mean number of jumps and force per jump with the corresponding distributions measured on consecutive days	6
Figure S5. Young’s modulus of the different ECM regions	7
Figure S6. Correlation between mean number of jumps and mean force per jump with Young’s modulus and protein composition	8
Figure S7. Optical image of the rat bladder ECM with the LMD cut	9
Figure S8. Distributions of jumps and tethers forces before and after the addition of the 4b4 integrin inhibitor antibody on AY-27 cells.....	10
Figure S9. Contact angle analysis of water on functionalised silicon substrates	11
Supporting Note SN1. Cleaning and re-use of the ECM probes	11
Supporting Movies SM1, SM2, SM3. Attachment of ECM pieces to functionalised cantilevers	11

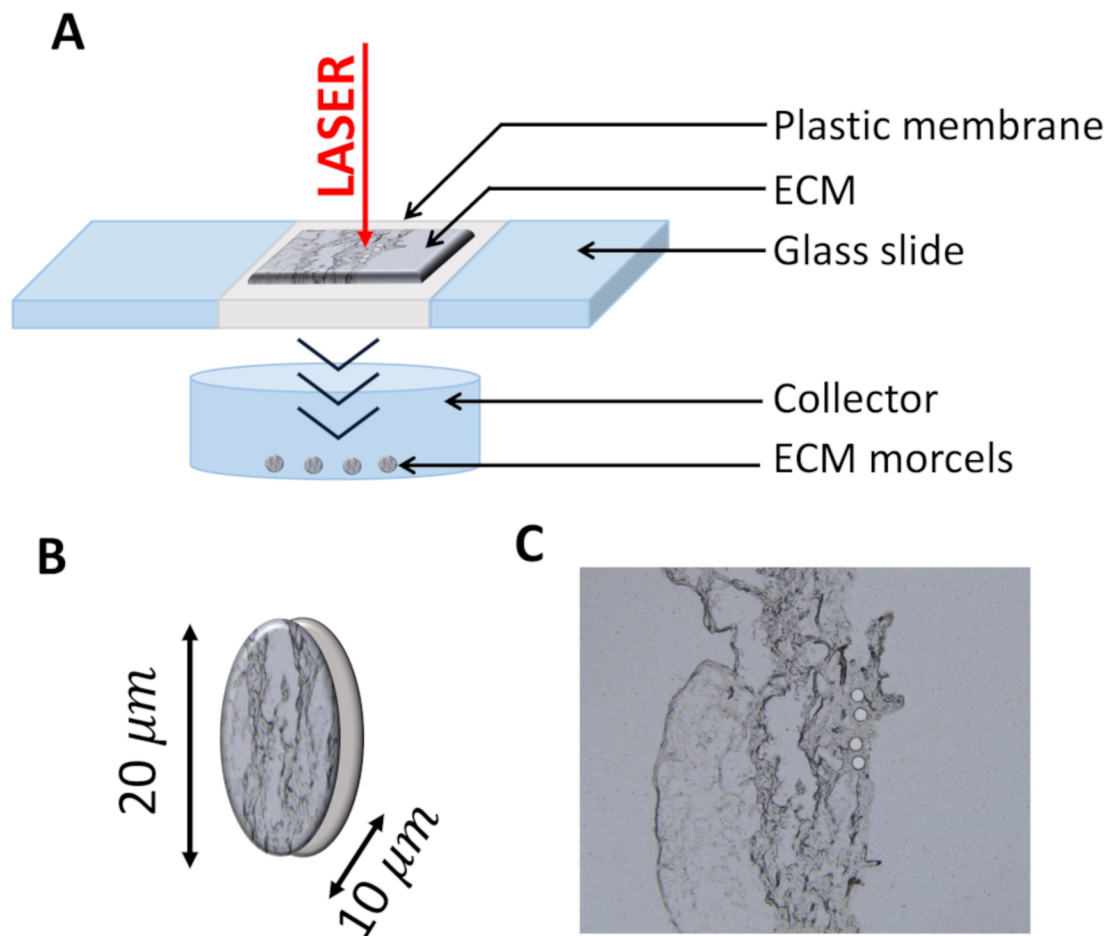


Figure S1. Schematics of the conventional use of the LMD system. (A) ECM fragments are cut by the UV laser together with the underlying plastic membrane and collected in a suitable reservoir where they fall by gravity. (B) The resulting circular pieces are 20 μm in diameter and 10 μm thick, excluding the plastic membrane. (C) Upon cutting and collecting the pieces, circular holes are left in the ECM slice.

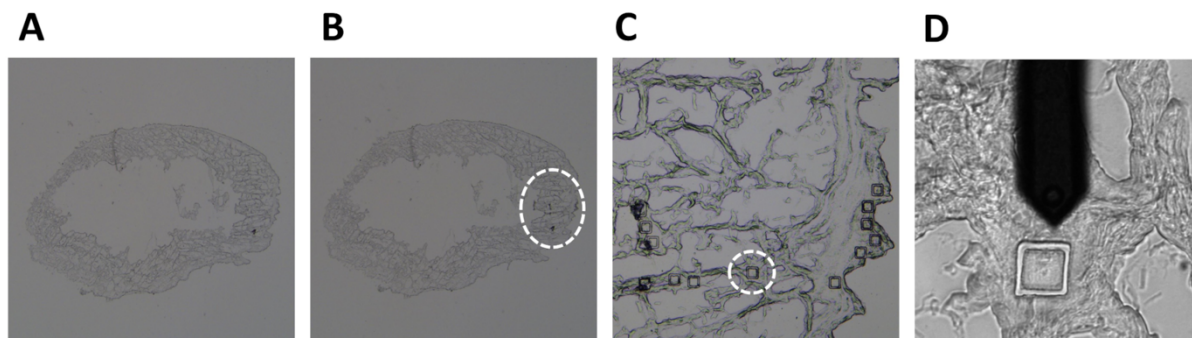


Figure S2. Optical images of the ECM rat bladder. (A) Before LMD cut, after PBS wash and ethanol dehydration. (B) After the LMD cut; the region of the cut is indicated. (C,D) Magnification of the cut region. The AFM cantilever is visible in D.

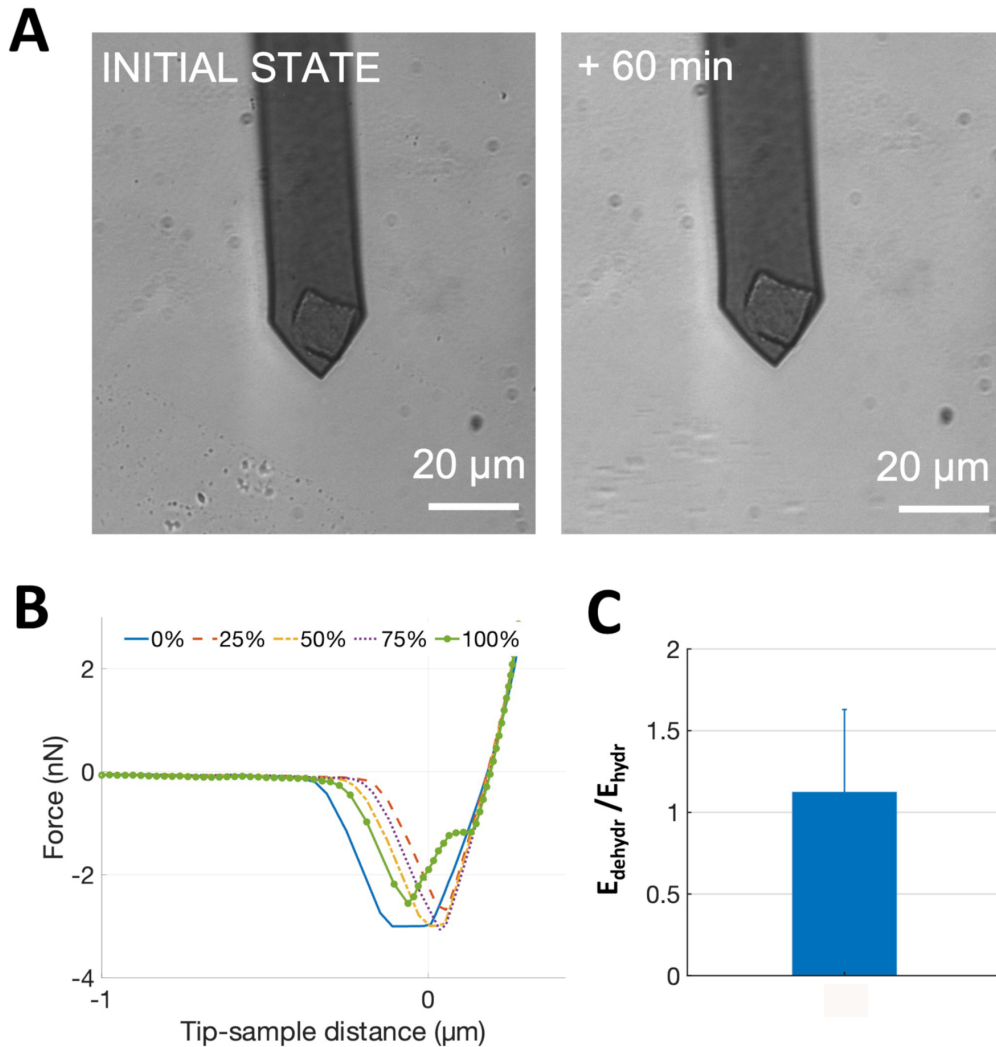


Figure S3. Stress tests on the ECM probes. (A) Optical images of an ECM probe before and after continuous scanning across a $20\mu\text{m} \times 20\mu\text{m}$ area in Contact Mode for 60 minutes on a glass surface with a scan frequency of 1Hz. (B) Representative retraction curves acquired using an ECM probe ramped against a glass substrate before (0%), during (25, 50 and 75%), and at the end (100%) of an adhesion force spectroscopy experiment consisting in the acquisition of a total of 400 FCs. (C) The ratio $E_{\text{dehydr}}/E_{\text{hydr}}$ of Young's modulus values E of an ECM sample before and after dehydration with 70% EtOH (the error bar represents the error calculated as the propagation of the effective standard deviations of the mean of E_{hydr} and E_{dehydr}).

Stress tests were performed to assess the firm attachment of the matrix to the cantilever and the force spectroscopy functionality after repeated use.

Firstly, we perform continuous scanning of a $20\mu\text{m} \times 20\mu\text{m}$ square on glass at a frequency of 1Hz with the probe for more than 60 minutes and observed no appreciable displacement or damage (Figure S3A). Then, we carried out force spectroscopy in liquid on a glass surface, with 10s contact time, by recording 400FCs at 1Hz with 5nN

applied force. Looking at representative FCs at the beginning (0%), during (25, 50 and 75%) and at the end of the experiment (100%), we did not notice important changes in the measured total adhesion force (Figure S3B) (a slight decrease can be noted at the end of the test, while no significant differences is observable in the first 75% of the test). Interestingly, in this case, where the ECM is interacting with a glass surface instead of a cell, we did not detect unbinding events (jumps and tethers) in the FCs, which are typically associated to integrin-related specific adhesive interactions.

Furthermore, as LMD requires the dehydration of the matrix with a minimum of 70% Ethanol, we performed AFM nanoindentation measurements on the same ECM before and after dehydration with Ethanol. No significant difference in the Young's modulus of the ECM was observed (Figure S3C).

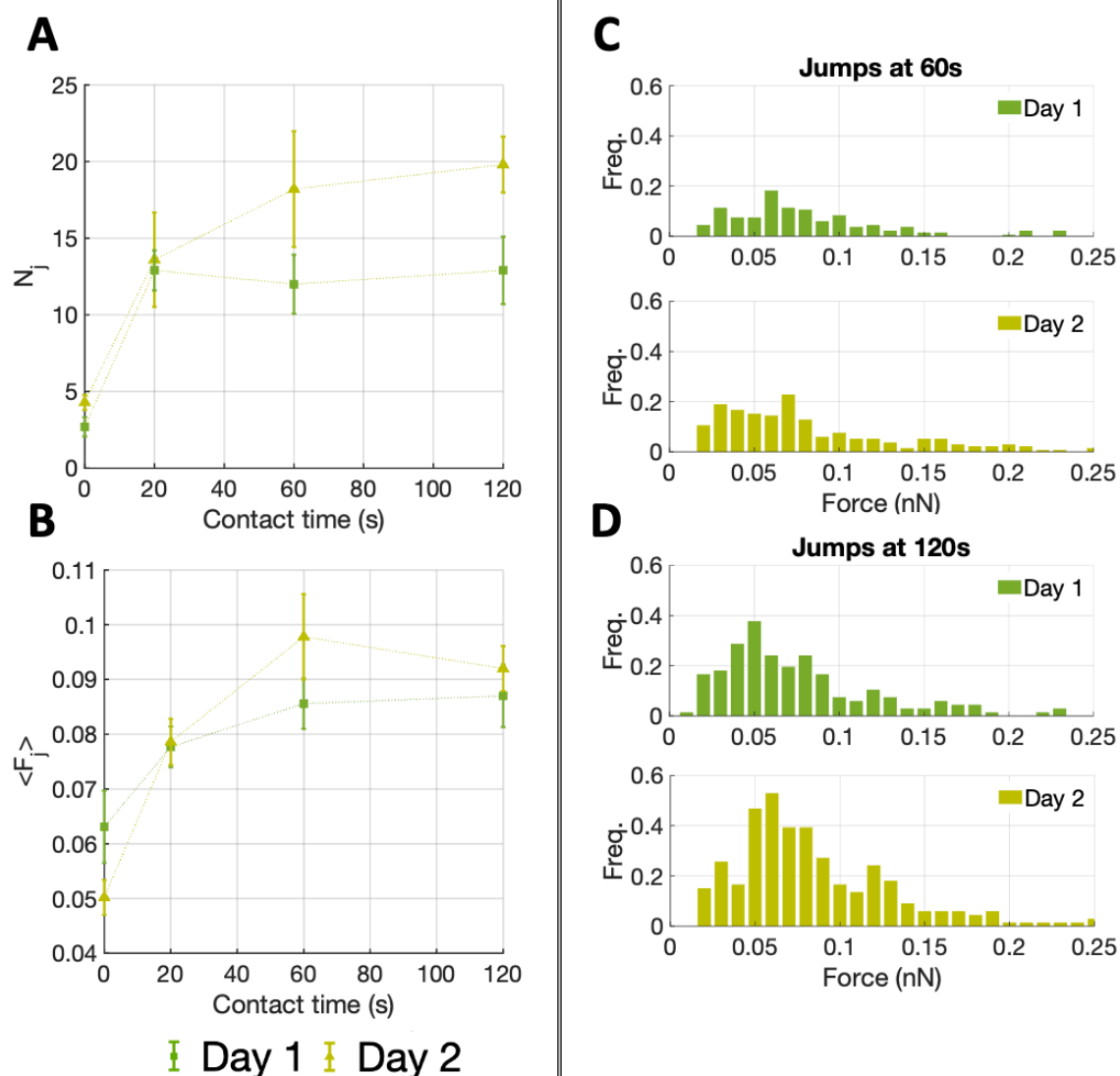


Figure S4. Mean number of jumps and force per jump with the corresponding distributions measured on consecutive days (boxes A and B, C and D, respectively), during adhesion force spectroscopy experiments performed with the same ECM probe on AY-27 cells from the same passage: day 1 (in dark green) and day 2 (in light). Different contact times (ct) have been used (ct = 0 s, 20 s, 60 s, 120 s). The distributions of the force of single jumps at two contact times are shown in (C) (ct=60s) and (D) (ct=120s).

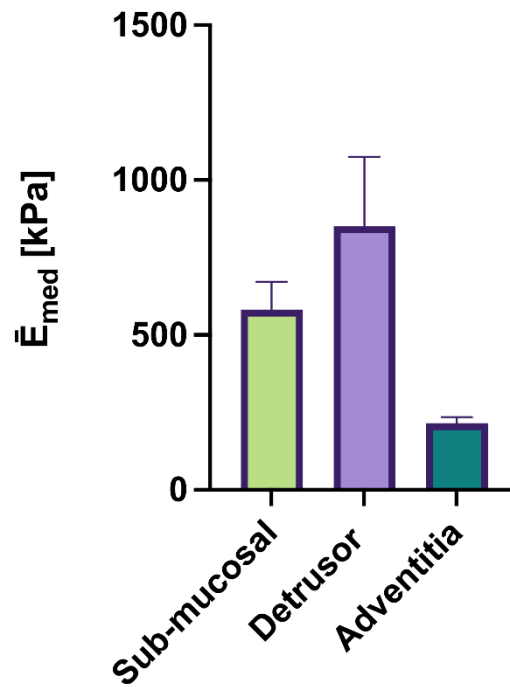
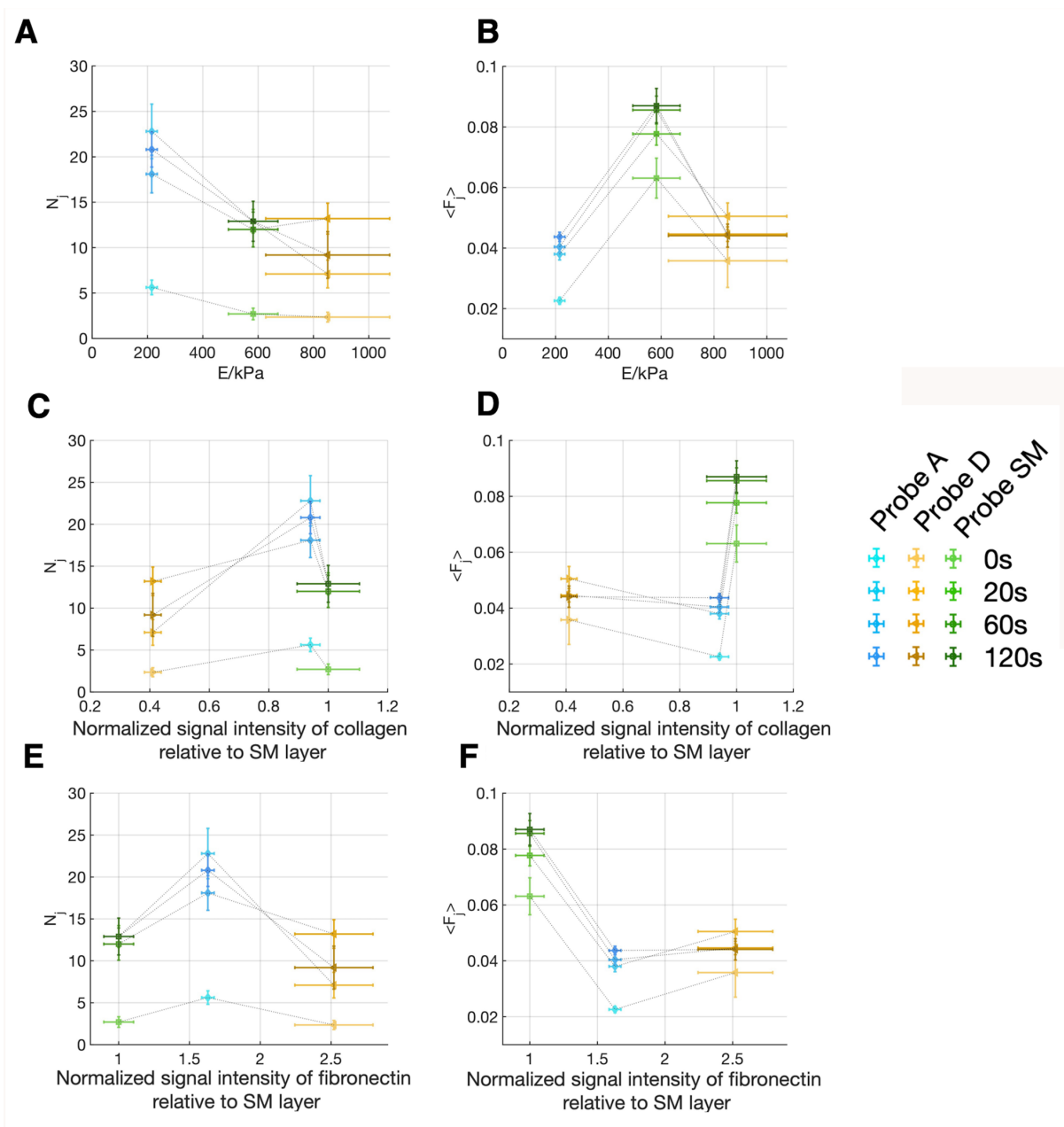


Figure S5. Young's modulus of the different ECM regions: sub-mucosal, detrusor and adventitia. The mean median values are reported; error bars represent standard deviations of the mean. Data have not been corrected for bottom effect and might therefore overestimate the true Young's modulus values. All measurements have been performed on the same 10 μ m decellularised ECM slice, on microdissected pieces (inside and outside taken as equivalent). Error bars represent the standard deviation of the mean.



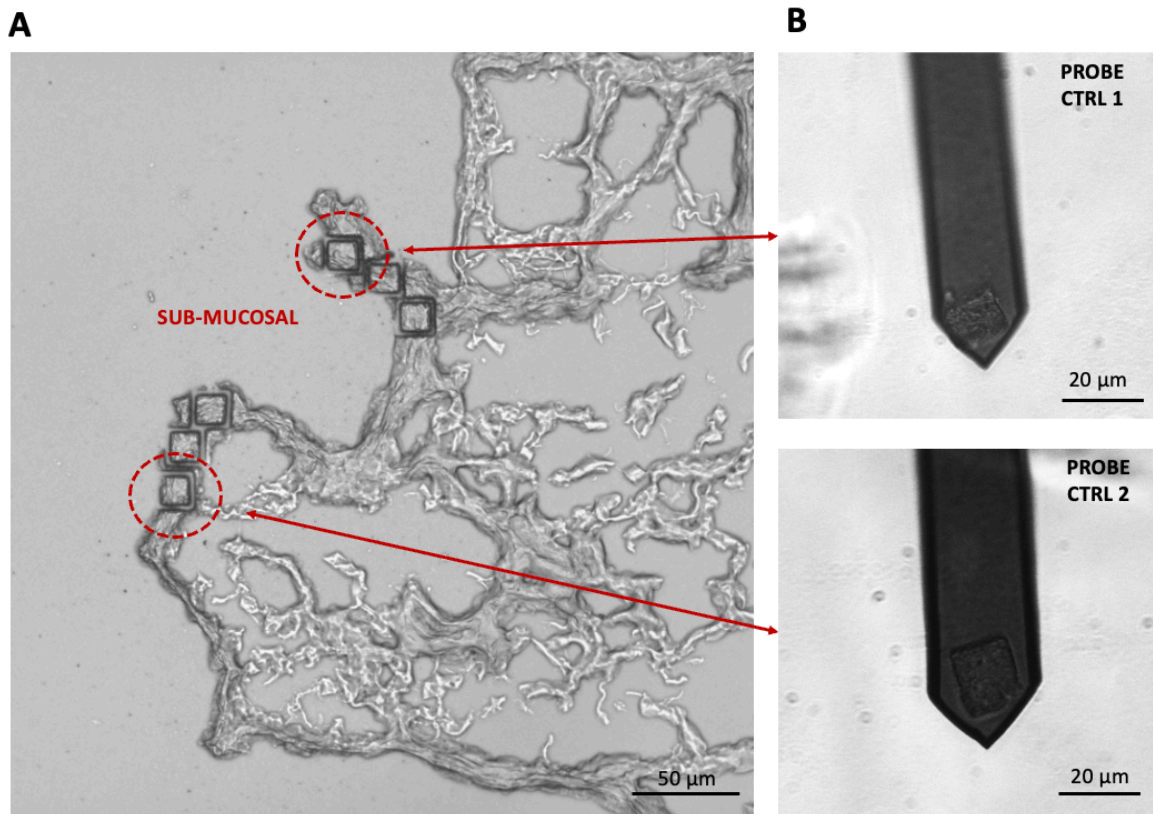


Figure S7. Optical image of the rat bladder ECM with the LMD cut. The red circles in (A) highlights the region in the submucosal layer where the ECM was cut to produce the control probes CTRL1 and CTRL2, shown in (B). The control probes were used in the integrin inhibitory experiments.

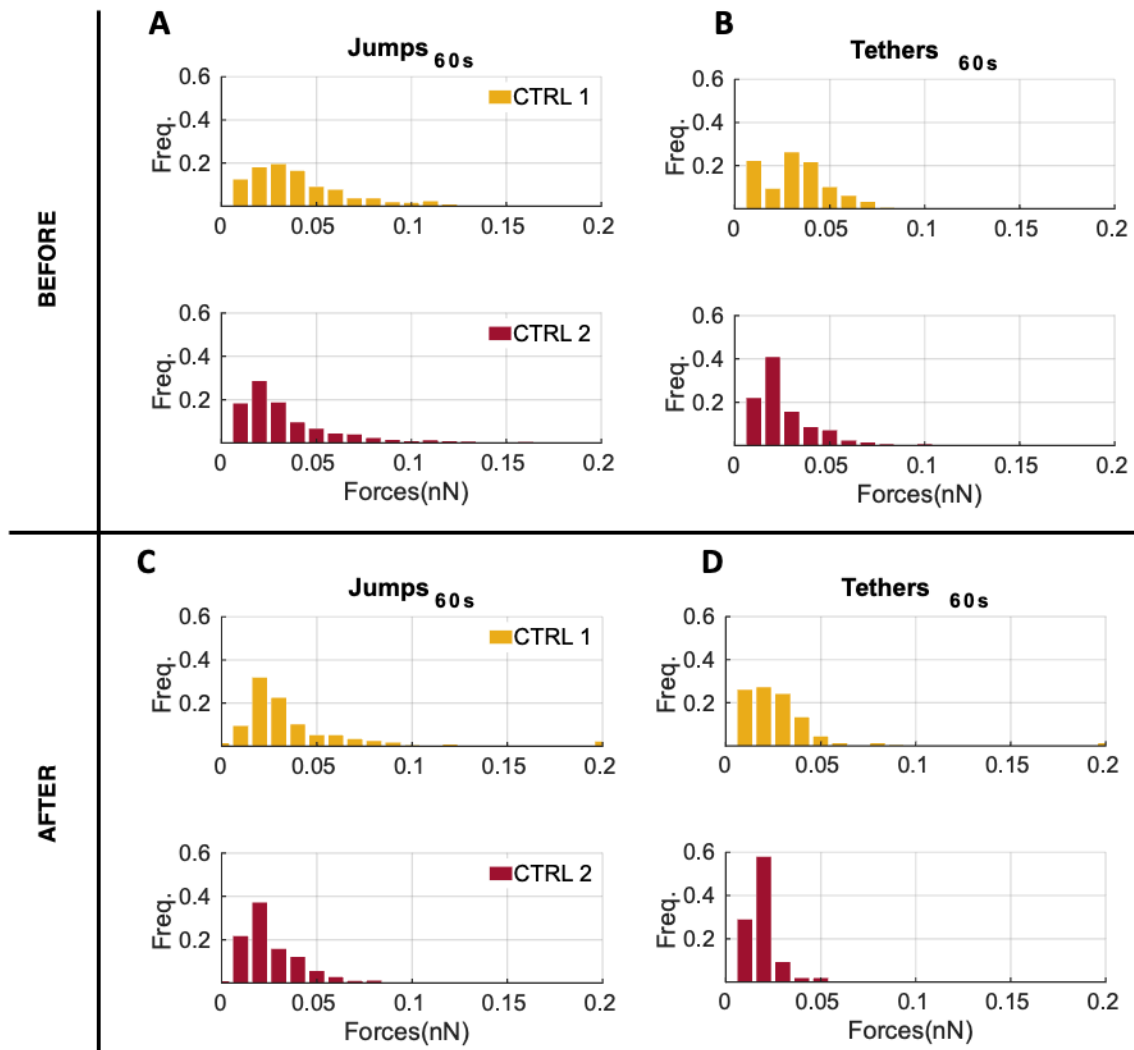


Figure S8. Distributions of jumps and tethers forces before and after the addition of the 4b4 integrin inhibitor antibody on AY-27 cells (boxes A-B and C-D, respectively), measured during control adhesion force spectroscopy experiments with $ct = 60s$ performed with the CTRL1 and CTRL2 probes (see Figure S6).

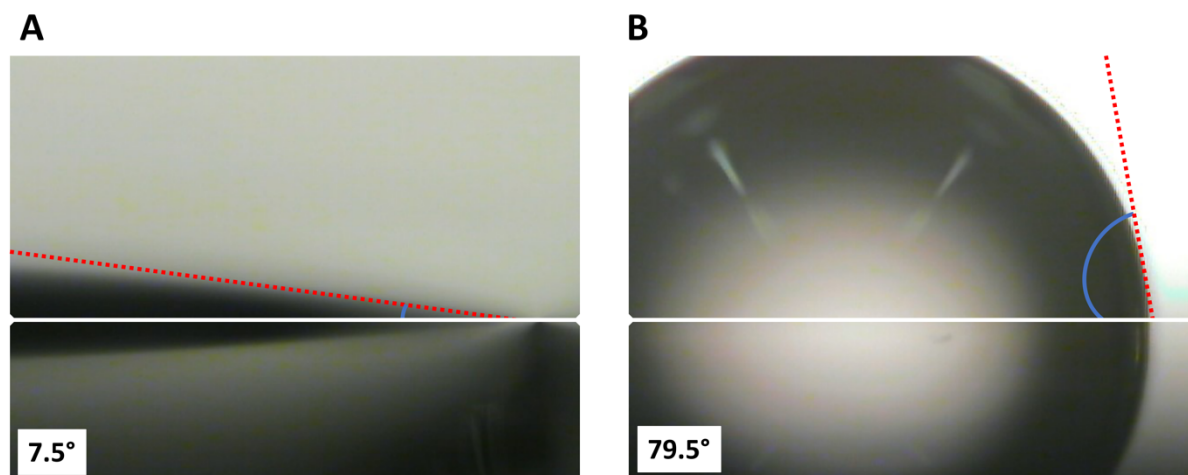


Figure S9. Contact angle analysis of water on functionalised silicon substrates, (A) before, and (B) after functionalisation with APTES. The contact angle increased from 7° to 79.5° upon APTES functionalisation of the oxidised silicon substrate.

Supporting Note SN1. Cleaning and re-use of the ECM probes

ECM probes can be cleaned and re-functionalised. In fact, the ECM can be degraded with proteolytic enzyme solutions such as helizyme, while the APTES coating (as well as the ECM) can be removed by piranha solution. Piranha solution is known to degrade any organic residues out of substrate such as silicon wafer and is commonly use in the AFM community for cleaning the probes.

Supporting Movies SM1, SM2, SM3. Attachment of ECM pieces to functionalised cantilevers